JACS
JOURNAL OF THE AMERICAN CHEMICAL SOCIETY

ARTICLE

pubs.acs.org/JACS

Subcomponent Self-Assembly and Guest-Binding Properties of Face-Capped $Fe_4L_4^{8+}$ Capsules

Rana A. Bilbeisi, Jack K. Clegg, Noémie Elgrishi, Xavier de Hatten, Marc Devillard, Boris Breiner, Prasenjit Mal,[†] and Jonathan R. Nitschke*

Department of Chemistry, University of Cambridge, Lensfield Road, Cambridge CB2 1EW, U.K.

Supporting Information

ABSTRACT: A general method for preparing Fe_4L_4 face-capped tetrahedral cages through subcomponent self-assembly was developed and has been demonstrated using four different C_3-symmetric triamines, 2-formylpyridine, and iron(II). Three of the triamines were shown also to form Fe_2L_3 helicates when the appropriate stoichiometry of subcomponents was used. Two of the cages were observed to have nearly identical Fe−Fe distances in the solid state, which enabled their ligands to be coincorporated into a collection of mixed cages. Only one of the cages combined a sufficiently large cavity with the sufficiently small pores required for guest binding, taking up a wide variety of guest species in size- and shape-selective fashion.

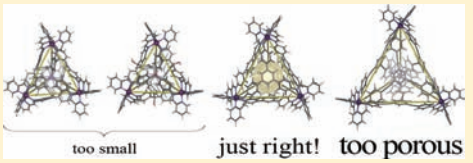

INTRODUCTION

Metal−organic capsules[1−10] have been demonstrated to be useful in a variety of contexts. These structures' selective guest encapsulation abilities show promise in separations of substrates as diverse as gases,[11] anions,[12,13] and fullerenes.[14−16] They also enable the reactivities of guests to be modulated,[17] allowing sensitive species to be protected from the environment[18−21] and species to be transformed via inner-phase[22] catalysis,[23−25] in a manner similar to natural systems. Many of these functions have been explored using a limited number of capsules, key examples being a $Pd_6L_4^{12+}$ capsule prepared by Fujita's group[26] and a $Ga_4L_6^{12-}$ species first reported by Raymond and co-workers.[27] These promising applications have created a need for straightforward and general methods for the creation of new host architectures. Herein we address this need through the development of a method for the preparation of $Fe_4L_4^{8+}$ face-capped tetrahedral cages[28−39] using the subcomponent self-assembly method,[40] by which complex structures may be prepared from simple building blocks through the formation of both dynamic-covalent[41] (C═N) and coordinative (N→M) linkages during the same overall self-assembly process.

Whereas in edge-linked M_4L_6 tetrahedral assemblies[13,27,28,42−47] ditopic ligands bridge pairs of metal centers, defining the twofold symmetry axes of a tetrahedron, face-capped M_4L_4 assemblies[28−39] incorporate tritopic ligands, which bridge three metal centers to define the tetrahedron's threefold symmetry axes. The portals of an edge-linked M_4L_6 tetrahedron thus lie on its four faces, whereas the corresponding openings in a face-capped M_4L_4 tetrahedron are found on its six edges. For a given ligand size, we reasoned that the six portals of an M_4L_4 tetrahedral framework should individually be smaller than the four apertures of an M_4L_6 congener, potentially providing a larger ligand surface area[48] and allowing the M_4L_4 host to enclose an inner cavity more effectively. More tightly closed-off cavities may lead to more effective guest binding. Despite the favorable guest-encapsulation properties of face-capped cages, fewer examples of guest encapsulation in these M_4L_4 species have been reported[30,31,49−52] compared with their edge-bridged M_4L_6 counterparts.

Scheme 1. General Procedure for the Subcomponent Self-Assembly of M_4L_4 Tetrahedral Cages: Triamines A−D, 2-Formylpyridine, and Iron(II) Salts Were Mixed in Acetonitrile To Yield the Corresponding Cages

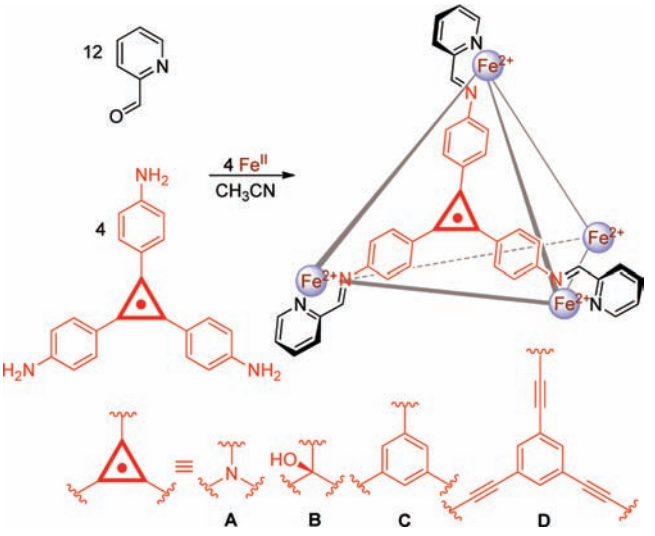

As shown in Scheme 1, the procedure developed here allowed the preparation of a new Fe_4L_4 cage from each of the four

Received: September 30, 2011
Published: November 01, 2011

Scheme 2. Preparation of $[Fe_4L_4]^{8+}$ Tetrahedron 1 via Subcomponent Self-Assembly

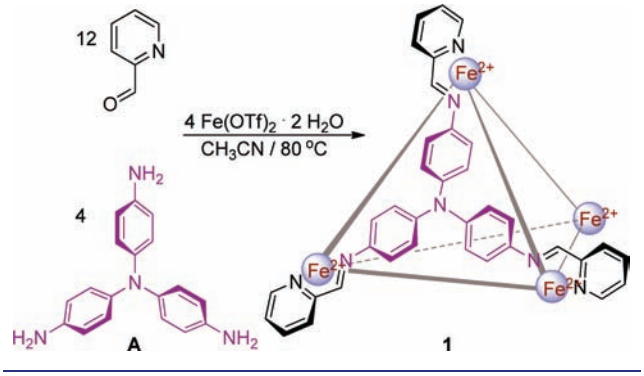

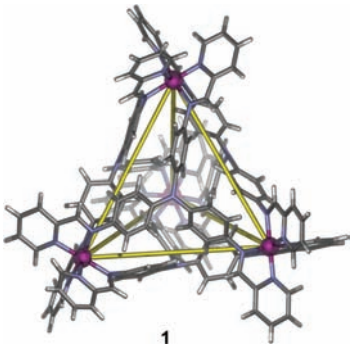

Figure 1. Cationic part of the crystal structure of cage **1**.

Scheme 3. Preparation of $[Fe_2L_3]^{4+}$ Helicate 2 from the Same Building Blocks Used To Prepare Cage 1

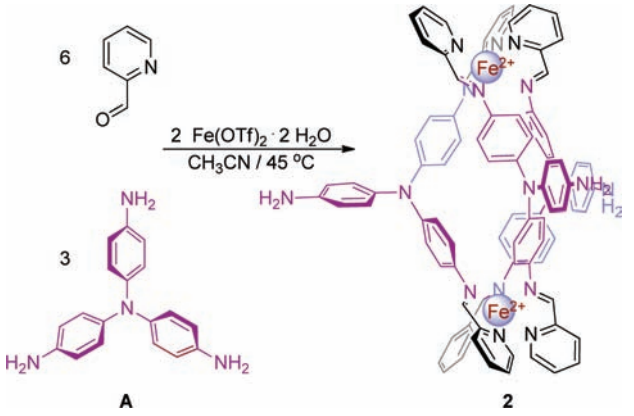

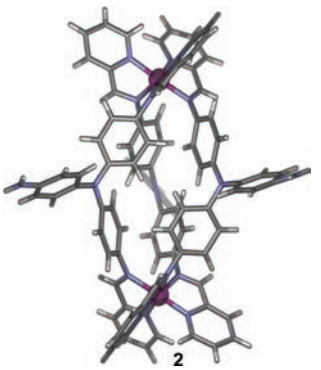

Figure 2. Cationic part of the crystal structure of helicate **2**.

C_3-symmetric trianilines investigated (**A**–**D**). The two smaller cages did not bind guests; calculations suggested that their cavity volumes were not large enough. Their subcomponent triamines **A** and **B** did show an unprecedented ability to form mixed-ligand cages, however. The largest cage, formed from **D**, also showed no guest binding, which we attribute to the cage's large pore windows, resulting in the cage's cavity being insufficiently isolated from the external environment to provide a suitable binding pocket for the guest molecules tested. The cage prepared from **C** combined an internal volume large enough for guest binding with smaller apertures, allowing for host–guest binding to be observed.

Whereas a wealth of different species having the general formula $M_{2n}L_{3n}$, including helicates and cubes, have been observed for the combination of bis-bidentate ligands with six-coordinate metals,[1,49,53−55] to our knowledge the present study is the first in which identical C_3-symmetric linkers have been employed to generate architectures containing differing numbers of building blocks. Through simple adjustments to the stoichiometry and reaction conditions used to form the Fe_4L_4 cages in this study, new Fe_2L_3 helicates could also be formed from subcomponents **A**, **C**, and **D**.

RESULTS AND DISCUSSION

The reaction of triamine **A** (4 equiv) with 2-formylpyridine (12 equiv) and iron(II) (4 equiv) yielded tetrahedral cage **1** (Scheme 2). Vapor diffusion of ethyl acetate into an acetonitrile solution of **1** gave crystals suitable for structure determination by single-crystal X-ray diffraction. A representation of the X-ray structure of **1**·8OTf·27MeCN is shown in Figure 1. Four octahedral iron(II) centers are bridged by four ligands, each of which caps a face of the tetrahedron. The iron(II) centers are separated by 11.9 Å. The volume of the central cavity was calculated to be 31 Å^3.[56] The central nitrogen atoms of each ligand are slightly pyramidalized, with C–N–C angles ranging from 112.9(7) to 120.5(8)° (mean ~117°). Cage **1** crystallizes with approximate T point-group symmetry, such that all of the iron(II) stereocenters within one cage share the same Δ or Λ stereochemistry. Both cage enantiomers are present in the crystal, related by inversion symmetry. The ligands bridging the metal centers also adopt a chiral propeller-like helical arrangement. Each of the ligands adopts the same chiral configuration as the metal centers that they bridge. This arrangement is similar to that observed in a number of related cage molecules.[49,57] The high symmetry of **1** is preserved in solution, as inferred from NMR analysis.

A simple change in stoichiometry gave triple helicate **2** (Scheme 3) from the same subcomponents used to prepare **1**. Vapor diffusion of ethyl acetate into an acetonitrile solution of **2** provided crystals suitable for single-crystal X-ray diffraction. The structure of **2**·4OTf·9MeCN is shown in Figure 2. The two iron(II) centers in **2** have the same stereochemistry, generating a structure with idealized D_3 symmetry. In contrast to **1**, only two of the amines from each residue of **A** condensed with 2-formylpyridine, leading to the formation of C_2-symmetric bis-bidentate ligands. The Fe^{II}–Fe^{II} distance is 11.3 Å, slightly shorter than in the structure of **1**. The central nitrogen atoms in

dx.doi.org/10.1021/ja2092272 |J. Am. Chem. Soc. 2012, 134, 5110–5119

Scheme 4. Subcomponent Self-Assembly of $[Fe_4L_4]^{8+}$ 3: (a) $4Fe(OTf)_2 \cdot 2H_2O$ in CH_3CN at 70 °C; (b) $4FeSO_4 \cdot 6H_2O$ in H_2O at 70 °C

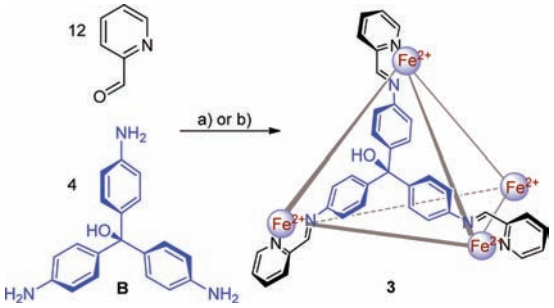

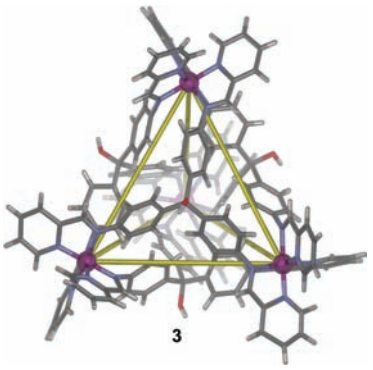

Figure 3. Cationic part of the crystal structure of cage **3**.

the ligands of **2** are more planar than those of **1**, with C−N−C angles in the range from 115.6(6) to 123.6(7)° (mean ∼120°).

When a 4:12:4 stoichiometry of **A**, 2-formylpyridine, and Fe^{II} was employed in the preparation of tetrahedron **1**, no **1** was observed after leaving the sample at 25 °C for a day. Only ^1H NMR resonances corresponding to **2** and unreacted starting materials were present, marking **2** as a kinetically stable intermediate product. Peaks corresponding to **1** appeared once the reaction mixture had been heated to 80 °C, however, and equilibration at this temperature for 11 days was observed to eliminate all other peaks (corresponding to helicate **2** and starting materials) from the ^1H NMR spectrum, leaving only the thermodynamic product **1**.

The use of tris(4-aminophenyl)methanol **B** as a building block enabled the formation of cage **3**, as shown in Scheme 4. In addition to the acetonitrile-soluble triflate salt of **3**, the water-soluble sulfate salt could be prepared by using ferrous sulfate in place of the triflate in an aqueous reaction medium; **3** was thus the only Fe_4L_4 complex described in this study that could be prepared in water-soluble form. This sulfate salt could be converted into the hexafluorophosphate salt through anion metathesis by adding a saturated aqueous potassium hexafluorophosphate solution dropwise to an aqueous solution of the sulfate salt of **3**.

NMR spectra were consistent with a *T*-symmetric solution structure for **3** analogous to that of **1**. Vapor diffusion of diethyl ether into an acetonitrile solution of the hexafluorophosphate salt of **3** gave crystals suitable for single-crystal X-ray diffraction analysis. A representation of the X-ray structure of $3 \cdot 8PF_6 \cdot 5MeCN \cdot 5C_4H_{10}O$ is shown in Figure 3. The four Fe^{II} centers are bridged by three C_3-symmetric ligands, resulting in a face-capped tetrahedral arrangement with idealized *T* symmetry similar to the structure of **1**. As expected, the ligands' central hydroxy-bearing carbon atoms are significantly more pyramidalized than the corresponding nitrogen atoms in **1**, with $C_{phenylene}-C(OH)-C_{phenylene}$ angles ranging from 102.5(12) to 115.2(13)° (mean ∼110°). Each hydroxyl group points outward, away from the center of the molecule. As with **1**, the propellers formed by the ligands also display the same handedness as the metal centers. Although the metal−metal distances in **3** (mean 11.8 Å) are similar to those in **1**, the calculated void volume of **3** (45 $Å^3$; see below) is nearly 50% greater. The outward puckering of the pyramidalized ligands of **3** in comparison with the more planar ligands of **1** allows **3** to enclose a larger volume.

In contrast to the behavior of the other triamines examined in this study, we observed no evidence for the formation of a helicate from triamine **B** when the corresponding M_2L_3 stoichiometry of building blocks was employed. Mixing iron(II) triflate (2 equiv) with 2-formylpyridine (6 equiv) and triamine **B** (3 equiv) in acetonitrile resulted in a dark-purple solution whose ^1H and ^{13}C NMR spectra were broad and complex. The NMR spectra of the sample after heating to 50 °C for 14 h contained only peaks corresponding to tetrahedron **3** and excess **B**. We attribute this result to the greater steric crowding of adjacent phenyl rings that would be required at the metal centers to allow the formation of a helix using **B**. Examination of an MM2-optimized molecular model[58] of a hypothetical helicate incorporating **B** based on the crystal structure of **2** suggested that the closest $H_{phenylene}-C_{phenylene}$ contact would be reduced from 2.75 Å in the case of **2** to 2.52 Å in an analogous helicate incorporating **B**, which is less than the sum of van der Waals radii for C and H (2.7 Å). Our model suggests that in this helicate, the pyramidal sp^3-hybridized central carbon of **B** would bring the adjacent phenyl rings into closer contact than is the case for subcomponent **A**, with its planar sp^2-hybridized central nitrogen atom. This closer arrangement of the phenylene rings in **B** appears to constrain the ability of each ring to adopt a configuration that avoids unfavorable steric interactions between phenylene rings around the Fe^{II} center and at the C−OH center of the ligand in a helicate formed from this subcomponent. Capsule **3** is thus the sole isolated product of the self-assembling system of **B**, 2-formylpyridine, and Fe^{II}, whereas either **1** or **2** may be selected as the product of the corresponding system containing **A**, depending on the stoichiometry of subcomponents employed.

The structural similarities of **1** and **3** and of **A** and **B** allowed the latter to be coincorporated into mixed-ligand cages, as shown in Scheme 5. No preference for either heteroleptic or homoleptic cages was observed: **A** and **B** appeared to be fully interchangeable, such that a statistical mixture of cages incorporating A_4 (i.e., cage **1**), A_3B, A_2B_2, AB_3, and B_4 (i.e., cage **3**) were formed in a 1:4:6:4:1 ratio, as observed by electrospray ionization mass spectrometry (ESI-MS) (Figure 4). NMR spectra of this mixture were complex, consistent with the lowered symmetries of the heteroleptic cages; signals corresponding to **1** and **3** were observed among many new ^1H signals.

The observation of mixed cages appeared to require a close structural correspondence between subcomponents: when mixed together in an analogous fashion as **A** and **B** in Scheme 5, any subset of **A**, **B**, **C**, and **D** that did not contain both **A** and **B** was observed to produce only homoleptic cages, indicating that the

Scheme 5. Preparation of Mixed-Ligand Cages Containing Subcomponents A and B; Purple and Blue Panels Represent A and B Residues, Respectively

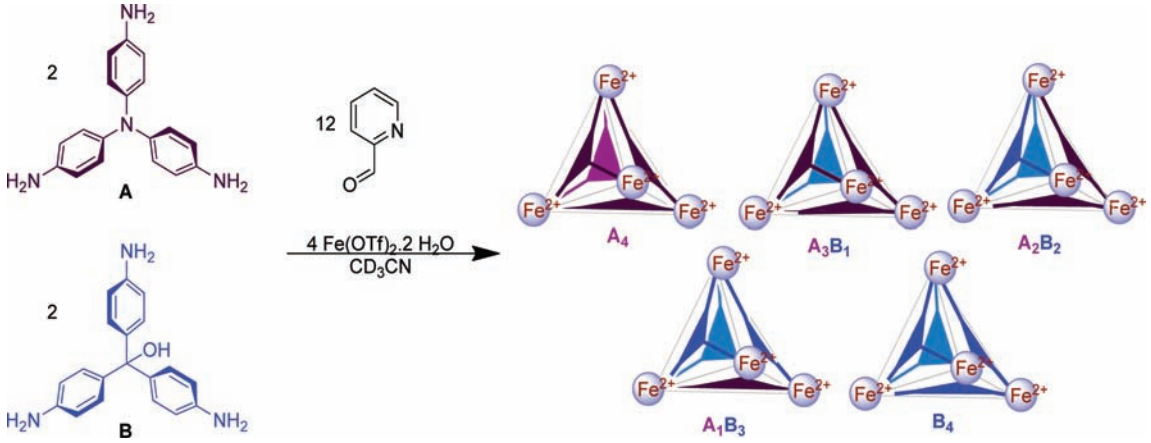

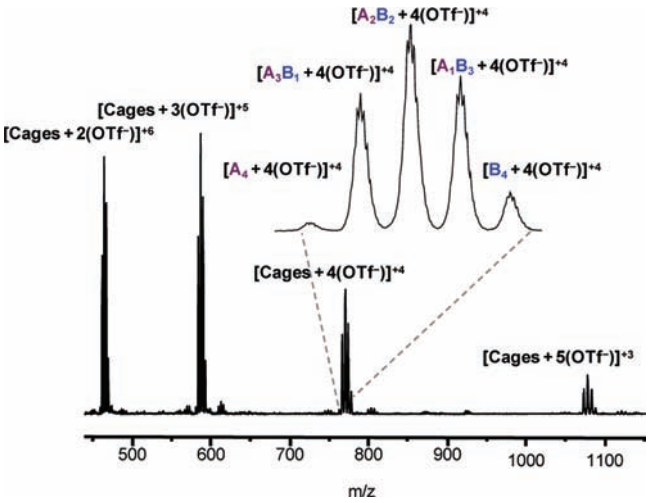

Figure 4. ESI mass spectrum of the mixed-ligand cage system of Scheme 5.

ligands underwent self-sorting,[59−66] as confirmed by ^{1}H NMR spectroscopy and ESI-MS.

As shown in Scheme 6, the cage-forming subcomponent self-assembly reaction could be extended to the preparation of capsule **4** from triamine **C**[67,68] in the presence of excess cyclohexane. As **C** is less soluble than **A** or **B**, a larger volume of solvent was required to avoid the formation of insoluble byproduct. We infer cyclohexane to have played a templating role in the formation of **4**, because without cyclohexane a mixture of **4** and helicate **5** (see below) resulted. Within host **4**, the encapsulated cyclohexane guest's ^{1}H NMR signal was observed at −0.56 ppm, 2 ppm upfield from that of free cyclohexane; other guests' ^{1}H signals showed similar shielding effects, which we attribute to the ring currents of the phenyl rings constituting the capsule's walls. Integration of the cage and guest ^{1}H NMR peaks indicated a ligand/guest ratio of 4:1, consistent with cage formation. Our attempts to grow crystals suitable for single-crystal X-ray diffraction measurements proved unsuccessful. However, the observation of the host−guest chemistry of **4** in solution provided further evidence for our assignment of its structure as a hollow

Scheme 6. Synthesis of the $[C_6H_{12}\subset Fe_4L_4]^{8+}$ Cage $[C_6H_{12}\subset 4]$ from Triamine C, 2-Formylpyridine, and Iron(II) in the Presence of Cyclohexane

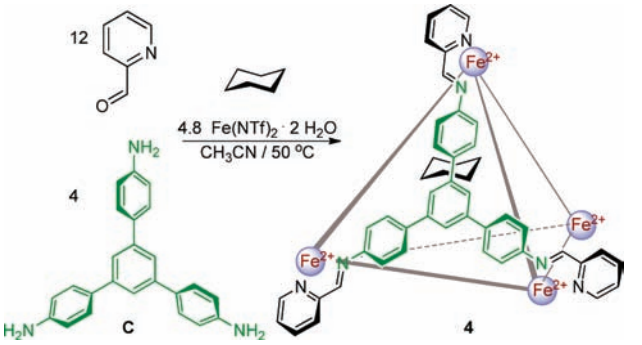

tetrahedron. This host−guest chemistry is discussed in detail in the next section. An MM2[58] model of **4** suggested a metal−metal separation of ∼14 Å and a substantial internal volume of 230 Å^3.

Again, changing the stoichiometry of the starting subcomponents allowed triple helicate **5** (Scheme 7) to be generated from the same subcomponents used to prepare **4**. We infer that the larger size of the ligands and the presence of the flat central phenylene spacer allow for the avoidance of the unfavorable steric interactions that were observed when the smaller triamine **B** was employed.

The even larger tetrahedron **6** could be prepared using triamine **D** (prepared in turn from the Sonogashira reaction between 1,3,5-tribromobenzene and 4-ethynylaniline), 2-formylpyridine, and iron(II) under conditions similar to those used to prepare structures **1**−**5** (Scheme 8). In this case, an excess of iron(II) salt (1.5-fold) was necessary to drive the reaction to completion. We attribute the requirement of excess metal to the more electron-deficient nature of subcomponent **D** (Hammett σ_p = 0.16 for −C≡CPh)[69] relative to subcomponents **C** (σ_p = −0.01 for −Ph)[69] and **B** (σ_p = −0.83 for −NMe$_2$);[69] previous studies[70,71] have demonstrated that electron-poor anilines lack the nucleophilicity necessary to drive imine formation to completion. The peaks in the ^{1}H NMR spectrum of **6** in acetonitrile (presented in the Supporting Information) were also broader than those of the other complexes reported herein, possibly

dx.doi.org/10.1021/ja2092272 |J. Am. Chem. Soc. 2012, 134, 5110–5119

Scheme 7. Preparation of $[Fe_2L_3]^{4+}$ Helicate 5 from the Same Building Blocks Used To Prepare Cage 4

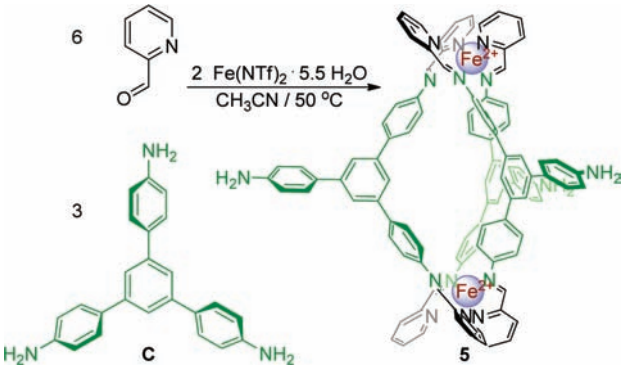

Scheme 8. Preparation of $[Fe_4L_4]^{8+}$ Tetrahedron 6 from Subcomponent D, 2-Formylpyridine, and Iron(II) Triflamide

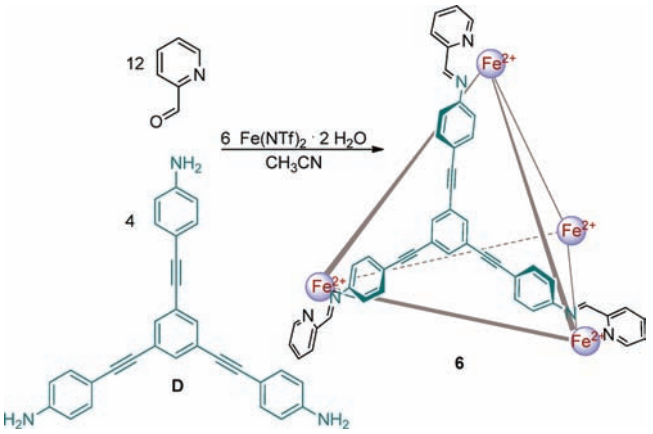

because of slower tumbling or interactions with a portion of this excess Fe^{II} in its high-spin state. No evidence of triflamide anion encapsulation was observed by ^{19}F NMR analysis, however; the ^{19}F signal of the triflamide anion (as measured against a hexafluorobenzene external standard) was observed to remain unchanged upon cage formation. An MM2 model of **6** suggested a metal−metal distance of ∼18.2 Å, reflecting the larger size of subcomponent **D**. The calculated void volume of 823 $Å^3$ places it among the largest reported volumes in related species.[16,72−74]

Helicate **7** was prepared cleanly upon mixing **D**, 2-formylpyridine, and Fe^{II} in the required 3:6:2 stoichiometry followed by equilibration for 12 h at 50 °C (Scheme 9). Although only signals corresponding to **7** could be identified in the ESI-MS spectrum, the NMR spectra were more complex than those of helicates **2** and **5**, containing two distinct sets of signals in a 76:24 ratio. Nuclear Overhauser effect spectroscopy (NOESY) and correlation spectroscopy (COSY) analyses were consistent with the presence of two diastereomeric forms of **7**. As has been previously reported,[55,75,76] ditopic ligands having sufficient flexibility can generate dinuclear structures in which the two metal centers have either the same stereochemical configuration (ΛΛ and ΔΔ) or opposing handedness (ΔΛ), generating an achiral meso structure. Although only the homochiral form of **7** is shown in Scheme 9, both diastereomers were inferred to be present in solution and to interconvert slowly on the NMR time scale.

Scheme 9. Preparation of $[Fe_2L_3]^{4+}$ Helicate 7 from the Same Subcomponents Used To Prepare 6

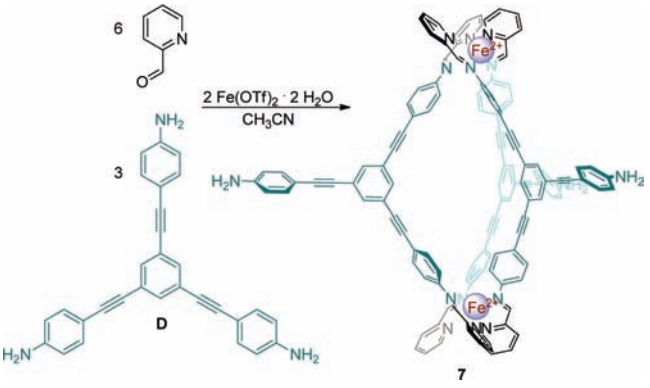

Within supramolecules containing multiple metal centers, the stereochemistry at one metal may influence another provided that the bridging ligands adopt conformations that are energetically distinct in the corresponding diastereoisomers.[49,52,57,74,77] This energetic differentiation was observed in cages **1**, **3**, **4**, **6** and helicates **2** and **5** to such a degree that only one diastereomer was observed in solution. The ligands thus provide effective stereochemical coupling between the metal centers, as reflected in the observations of the propeller-like gearing together of the phenyl groups of the ligands in the crystal structures of **1** and **3**. The alkynyl groups of **D**, in contrast, insulate the terminal phenyl rings from stereochemically coupling with the other parts of the ligands,[74,78−80] allowing the racemic and meso forms of **7** to coexist at similar energies.

Host−Guest Studies. The guest encapsulation properties of tetrahedral capsules **1**, **3**, **4**, and **6** were investigated in solution. Only **4** was observed to bind guests, as detailed below. The calculated volumes of **1**, **3**, **4**, and **6** reflect the sizes and shapes of the subcomponents employed (Figure 5). These volume determinations serve as points of reference in the discussion below.

No evidence for guest binding was observed by ^1H NMR spectroscopy following the addition to an acetonitrile solution of **1** or **3** (6.5 mM) of either (1) the tetrabutylammonium salt of F^-, Cl^-, Br^-, I^-, BF_4^-, NO_3^-, ClO_4^-, or PF_6^- (2.0 equiv in each case), (2) CH_2Cl_2, $CHCl_3$, CCl_4, or cyclopentane (5.0 equiv), or (3) He, Ne, Ar, CH_4, N_2O, CO_2, Xe, or SF_6 by bubbling the gas through the acetonitrile solution for 5 min at 25 °C.

We attribute the observed lack of guest binding by **1** and **3** to the small sizes of their cavities. The only neutral prospective guests that are sufficiently small are gases under practical experimental conditions. Even methane, however, would occupy 107% of the calculated volume of **1** or 74% of the volume of **3**, whereas the optimum occupancy for a gas has been estimated to be 40% of a container molecule's volume.[81] Neon, which would occupy 45% of **1** or 31% of **3**, and helium, for which the occupancies would be 37% and 25%, respectively, were also not observed to bind, possibly because of the weakness of the van der Waals interactions involving these monatomic gases or their low solubilities in the solvent employed.[82] Although all four halides would fit within **3** and fluoride, chloride, and bromide occupy less volume than the cavity of **1**, we observed no evidence for halide binding within either host. This lack of affinity may be due to the absence of specific, directional binding interactions, such as inwardly directed hydrogen-bond donors.[83−85]

dx.doi.org/10.1021/ja2092272 |J. Am. Chem. Soc. 2012, 134, 5110–5119

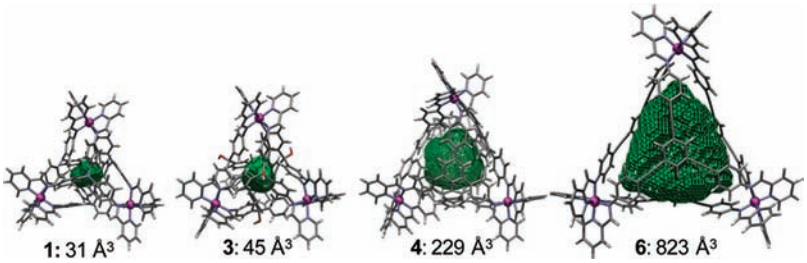

Figure 5. Crystal structures (**1** and **3**) and MM2 models (**4** and **6**) of the cages with their void volumes given and shown in green mesh.[56]

Table 1. Guests Explored for Cage 4

guest	volume (Å^3)[a]	encapsulation observed?
cyclohexane	111.5	yes
cyclohexene	107.8	yes
cyclopentane	70.7	yes
cyclopentene	90.7	yes
cyclohexanone	114.3	yes
cyclohexanol	119.1	yes
1-methylcyclopentanol	120.5	yes
benzene	99.5	yes
pyridine	92.8	yes
isoxazole	70.7	yes
toluene	117.4	no
n-pentane	106.5	no
carbon tetrachloride	88.7	yes
chloroform	74.7	yes
dichloromethane	60.9	yes
PF_6^-	74.7	no
ClO_4^-	54.8	precipitation
BF_4^-	53.7	no
I^-	34.8	no
Br^-	28.1	no
Cl^-	23.7	no
F^-	14.6	no
n-octane	161.9	no
1,3,5-trifluorobenzene	113.1	no
methylcyclohexane	129.7	no
o-xylene	135.1	no
m-xylene	135.6	no
cyclooctane	146.5	no
adamantane	159.0	no
naphthalene	151.0	no

[a] van der Waals volumes calculated from structures optimized using SPARTAN'10 with MP2 using a 6-311+G** basis set.[86]

To investigate the scope of guest binding within **4**, the molecules and anions listed in Table 1 were screened as potential guests. For each entry, the prospective guest (6 equiv for neutral guests and 3 equiv for the tetrabutylammonium salts of the anions) was added to an equilibrated solution of host **4** and **5** (6 mM) prepared from **C**, 2-formylpyridine, and iron(II) in the absence of cyclohexane as described above. For all of the ^{1}H NMR-active guests, signal(s) corresponding to the free guest were observed in the ^{1}H NMR spectrum. In cases where no encapsulation was inferred to have taken place, the signals for **4** appeared at the same chemical shifts as in the absence of the guest. Where host occupation was inferred, either a new set of cage and guest peaks were observed at different chemical shifts along with the sets of peaks corresponding to free **4** and guest, or new cage and guest peaks were observed together with those of excess free guest, while the peaks corresponding to the free host disappeared.

In a second round of experiments aimed at probing the relative binding strengths of the guests inside the cavity of **4**, each of the guests observed to bind during the preliminary studies (Table 1) was added to a solution of $[C_6H_{12}\subset\mathbf{4}]$ prepared as shown in Scheme 6, and the results were monitored by ^{1}H NMR spectroscopy. This series of experiments allowed a hierarchy of guest binding strengths to be established. For example, the addition of cyclopentane to the $[C_6H_{12}\subset\mathbf{4}]$ solution resulted in the formation of a mixture of $[C_6H_{12}\subset\mathbf{4}]$ and $[C_5H_{10}\subset\mathbf{4}]$, as indicated by ^{1}H NMR analysis. New sets of cage peaks were observed corresponding to both $[C_6H_{12}\subset\mathbf{4}]$ and $[C_5H_{10}\subset\mathbf{4}]$, along with encapsulated guest peaks at −0.57 and −0.50 ppm for cyclohexane and cyclopentane respectively. The relative ratios of the species present could be quantified by integration of the imine peaks at 9.89 and 10.05 ppm of $[C_6H_{12}\subset\mathbf{4}]$ and $[C_5H_{10}\subset\mathbf{4}]$, respectively (Table S1 in the Supporting Information). More weakly binding guests such as isoxazole, dichloromethane, chloroform, cyclohexanone, and 1-methylcyclopentanol were not observed to displace cyclohexane. On the basis of each guest's ability to displace cyclohexane within **4**, the relative binding strengths were determined to be CCl_4 > cyclohexene > cyclopentane > cyclohexane > pyridine > cyclopentene> cyclohexanol > benzene ≫ isoxazole, CH_2Cl_2, $CHCl_3$, and 1-methylcyclopentanol. The guest/cyclohexane ratios presented in Table S1 approximate the binding constants of the different guests relative to cyclohexane. The absolute values of guest binding constants could not be determined because of the templation role played by the guest in the formation of host **4**.

Collectively, these experiments reveal several trends in guest binding within the cavity of **4**. The strongly bound guests carbon tetrachloride, cyclopentene, cyclohexane, cyclopentane, cyclohexene, pyridine, and benzene are compact molecules with similar molecular volumes, suggesting that the range 88−112 Å^3 is optimal for encapsulation. These molecules all occupy slightly less volume than the 55% optimum observed for other host−guest systems.[87] The weaker binding of isoxazole marks this heterocycle as among the smallest guests tolerated, whereas 1-methylcyclopentanol appears to be among the largest.

Guests containing polar functional groups, such as isoxazole, cyclohexanone, and cyclohexanol, were weaker binders in **4**, whereas our previously reported water-soluble $Fe^{II}_4L_6$ cage[88] was observed to bind suitably sized heterocyclic guests, but none incorporating carbonyl or hydroxyl groups. This differential selectivity may be attributed to the greater importance of solvophobic (hydrophobic) effects in guest binding in the case of the $Fe^{II}_4L_6$ cage.[88]

dx.doi.org/10.1021/ja2092272 |*J. Am. Chem. Soc.* 2012, 134, 5110–5119

Neither *n*-pentane nor higher *n*-alkanes up to *n*-octane were observed to bind within **4** because of the entropic penalty that would be incurred during binding: a linear alkane must give up several degrees of freedom in order to coil up into a compact structure[89,90] similar to those of the cycloalkanes that were observed to bind well.

Cage **4** is thus one of the few tetrahedral cages that can encapsulate neutral guests containing polar functional groups in a nonaqueous solvent.[45,70,72,73,91−93] Although the hydrophobic effect is a useful driver of guest binding,[94] the water solubility of molecules containing polar functional groups limits such molecules' binding affinities in aqueous systems. The ability of capsule **4** to bind such polar guests (provided a size and shape fit exists) renders it useful in a complementary way to aqueous encapsulants.[11,17,20,94−96]

Cage **6** was also screened for guest binding by the addition of the guests listed in Table 1 under conditions identical to those used for cage **4**. In addition, the larger guests anthracene, ferrocene, decamethylferrocene, and decalin were also tested under these conditions. No evidence was observed for the formation of host−guest adducts that were stable on the ^{1}H NMR time scale at room temperature; spectra of **6** in solution with each prospective guest were superimposable upon spectra of the free host and guest (for ^{1}H NMR-active guests). We attribute this observation to the larger sizes of the open pores on the faces of cage **6** in comparison with cage **4**. Examination of MM2 models[86] revealed that the largest sphere that could freely pass through the pores of **6** would have a radius of 2.3 Å (larger objects could pass following slight deformation), whereas the pores of **4** have radii of only 1.3 Å, and the shorter Fe−Fe distances of **4** would be expected to render pore-opening deformations more energetically costly. We envisage that a comparison of pore sizes and guest cross sections may have predictive value in determining whether a binding event may take place. Future comparative studies will investigate this parameter in greater depth.

CONCLUSIONS

This study has demonstrated the applicability of the subcomponent self-assembly approach[40] to the generation of new face-capped tetrahedral Fe_4L_4 cages, complementing our demonstrations of the use of this technique in the construction of edge-linked tetrahedral Fe_4L_6 and face-capped cubic Fe_8L_6 assemblies.[16,20,70,74] This technique allowed the straightforward exploration of building blocks with different geometries, and both flat (**A**, **C**, and **D**) and pyramidalized (**B**) trianilines with different sizes were found to work well, suggesting that this method could be used to prepare Fe_4L_4 cages of various sizes from a range of other C_3-symmetric triamines.

The flat trianilines could be used to prepare M_2L_3 helicates as well as cages upon a simple change in stoichiometry, but pyramidalized trianiline **B** could not form helicates because of geometrical constraints. The ability to access helicates as well as cages from a given set of building blocks highlights a strength of the subcomponent self-assembly approach, which is shared by other methods where different kinds of bonds are formed during the same overall self-assembly process:[38,97] different structures may lie latent in the same collection of building blocks, separately accessible if the rules governing their stabilities are understood.

The parameters governing guest binding were explored, with only cage **4** fulfilling the criteria of being sufficiently large and sufficiently well-enclosed to exhibit the function[98] of guest binding. A hierarchy of binding strengths was established for a series of organic guest molecules. The novel observation that triamines **A** and **B** are capable of generating collections of mixed cages opens the possibility of creating dynamic combinatorial libraries[99,100] of larger mixed-panel cages. The presence of a suitable guest in solution could induce the templation of a host that can bind specifically to the chosen guest.[101] This dynamic host templation phenomenon is currently under investigation, along with binding studies of biologically relevant organic anions within cages accessible through the methods detailed herein.

EXPERIMENTAL SECTION

General Methods. Unless otherwise specified, all starting materials were purchased from commercial sources and used as supplied. Manipulations were performed under normal atmospheric conditions unless otherwise noted. NMR spectra were recorded on Bruker Avance DPX400 and Avance BB500 spectrometers; δ_H values are reported relative to acetonitrile-d_3 at 1.94 ppm unless otherwise noted. Low-resolution ESI-MS was performed on a Micromass Quattro LC instrument infused from a Harvard syringe pump at a rate of 10 μL/min. The compounds 1,3,5-tris(4′-aminophenyl)benzene (**C**)[49] and 4,4′,4″-(benzene-1,3,5-triyltris(ethyne-2,1-diyl))trianiline (**D**)[67] were prepared as described in the literature.

Preparation of [1](OTf$_2$)$_8$·8C$_4$H$_8$O$_2$. To a Teflon-capped J-Young NMR tube were added tris(4-aminophenyl)amine (**A**; 2.90 mg, 10 μmol, 4 equiv), 2-formylpyridine (2.85 μL, 30 μmol, 12 equiv), iron(II) triflate (3.54 mg, 10 μmol, 4 equiv), and deuterated acetonitrile (0.5 mL). The solution was degassed by three evacuation/nitrogen-fill cycles. The tube was kept at 80 °C overnight. [**1**](OTf)$_8$ was precipitated as a purple powder by the addition of ethyl acetate. ^{1}H NMR (400 MHz, 298 K, CD_3CN): δ 10.04 (12H, s, imine), 8.83 (12H, d, J = 7.6 Hz, 3-pyridine), 8.28 (12H, t, J = 7.72 Hz, 4-pyridine), 8.15 (12H, bs, 6-pyridine), 8.05 (12H, t, J = 5.6 Hz, 5-pyridine), 6.87 (24H, d, phenyl of the amine arms), 5.74 (24H, d, phenyl of the amine arms). ^{13}C NMR (100 MHz, 298 K, CD_3CN): δ 86.58, 114.58, 126.06, 134.34 (triflate anion), 140.61, 149.68, 151.30, 156.80, 157.26, 169.77, 172.62. ESI-MS: m/z 458.56 [**1**(OTf)$_2$]$^{6+}$, 580.26 [**1**(OTf)$_3$]$^{5+}$, 762.63 [**1**(OTf)$_4$]$^{4+}$, 1066.44 [**1**(OTf)$_5$]$^{3+}$, 1674.36 [**1**(OTf)$_6$]$^{2+}$. Elemental analysis of [**1**](OTf)$_8$ (%): Calcd for $C_{152}H_{108}F_{24}Fe_4N_{28}O_{24}S_8$·8$C_4H_8O_2$: C, 50.79; H, 3.98; N, 9.01. Found: C, 50.98; H, 4.19; N, 8.89.

Preparation of [2](OTf)$_8$. To a Teflon-capped J-Young NMR tube were added **A** (2.90 mg, 10 μmol, 3 equiv), 2-formylpyridine (1.90 μL, 20 μmol, 6 equiv), iron(II) triflate (2.35 mg, 6.67 μmol, 2 equiv), and deuterated acetonitrile (0.5 mL). The solution was degassed by three evacuation/nitrogen-fill cycles. The tube was kept at 45 °C overnight. ^{1}H NMR (400 MHz, 298 K, CD_3CN): δ 8.81 (6H, s, imine), 8.44 (6H, d, J = 7.6 Hz, 3-pyridine), 8.30 (6H, t, J = 7.6 Hz, 4-pyridine), 7.67 (6H, t, J = 6.3 Hz, 5-pyridine), 7.30 (6H, d, J = 7.30 Hz, 6-pyridine), 6.90 (6H, d, J = 7.2 Hz, phenyl of the amine arms), 6.79 (6H, d, J = 7.9 Hz, phenyl of the amine arms), 6.75 (6H, d, J = 8.4 Hz, triamine), 6.58 (6H, d, J = 8.1 Hz, triamine), 5.63 (6H, d, J = 7.0 Hz, triamine), 5.27 (6H, d, J = 7.6 Hz, triamine). ^{13}C NMR (125 MHz, 298 K, CD_3CN): δ 175.15, 158.72, 156.07, 150.25, 149.3, 146.53, 145.43, 139.93, 137.44, 135.51, 131.49, 129.99, 127.54. ESI-MS: m/z 379.12 [**2**]$^{4+}$, 555.15 [**2**(OTf)]$^{3+}$, 907.20 [**2**(OTf)$_2$]$^{2+}$.

Preparation of [3](SO$_4$)$_4$. To a Teflon-capped J-Young NMR tube were added tris(4-aminophenyl)methanol (**B**; 4.06 mg, 13 μmol, 4 equiv), 2-formylpyridine (3.8 μL, 40 μmol, 12 equiv), iron(II) sulfate heptahydrate (3.58 mg, 40 μmol, 4 equiv), and D_2O (0.5 mL). The solution was degassed by three evacuation/nitrogen-fill cycles. The tube was kept at 70 °C overnight. [**3**](SO$_4$)$_4$ was precipitated as a purple powder by the addition of isopropanol. ^{1}H NMR (400 MHz, 298 K, D_2O, with *tert*-butyl alcohol as a reference for peak assignments): δ 8.83

(12H, s, imine), 8.53 (12H, d, J = 5.9 Hz, 3-pyridine), 8.38 (12H, t, J = 7.6 Hz, 4-pyridine), 7.73 (12H, br, 5-pyridine), 7.58 (12H, br, phenyl of the triamine), 7.37 (12H, d, J = 4.0, 6-pyridine), 6.66 (12H, br, phenyl of the triamine), 5.94 (12H, br, phenyl of the triamine), 5.30 (12H, br, phenyl of the triamine). ^{13}C NMR (125 MHz, 298 K, D_2O, with *tert*-butyl alcohol as a reference for peak assignments): δ 80.98, 128.38, 129.54, 138.67, 139.76, 145.86, 149.94, 150.10, 155.53, 157.80, 175.90. ESI-MS: m/z 435.0 $[\mathbf{3}(SO_4)]^{6+}$, 676.20 $[\mathbf{3}(SO_4)_2]^{4+}$.

Preparation of [3](OTf)$_8$. To a Teflon-capped J-Young NMR tube were added **B** (4.06 mg, 13 μmol, 4 equiv), 2-formylpyridine (3.8 μL, 40 μmol, 12 equiv), iron(II) triflate (4.57 mg, 40 μmol, 4 equiv), and deuterated acetonitrile (0.5 mL). The solution was degassed by three evacuation/nitrogen-fill cycles. The tube was kept at 70 °C overnight. ^{1}H NMR (400 MHz, 298 K, CD_3CN): δ 8.62 (12H, s, imine), 8.55 (12H, d, J = 7.32 Hz, 3-pyridine), 8.36 (12H, t, J = 7.64 Hz, 4-pyridine), 7.74 (12H, t, J = 6.60 Hz, 5-pyridine), 7.56 (12H, br, phenyl of the triamine), 7.30 (12H, d, J = 5.3 Hz, 6-pyridine), 6.66 (12H, br, phenyl of the triamine), 5.79 (12H, br, phenyl of the triamine), 5.21 (12H, br, phenyl of the triamine), 4.78 (4H, s, methylhydroxyl at the center of the triamine). ^{13}C NMR (125 MHz, 298 K, CD_3CN): δ 176.42, 158.39, 156.10, 150.14, 147.04, 141.06, 139.99, 131.66, 114.6, 80.92. ESI-MS: m/z 468.4 $[\mathbf{3}(OTf)_2]^{6+}$, 591 $[\mathbf{3}(OTf)_3]^{5+}$, 777.6 $[\mathbf{3}(OTf)_4]^{4+}$, 1086.4 $[\mathbf{3}(OTf)_5]^{3+}$.

Preparation of [3](PF$_6$)$_8$·10H$_2$O. To a solution of $[\mathbf{3}](SO_4)_4$ in water was added dropwise a saturated aqueous potassium hexafluorophosphate solution. A purple solid precipitated and was collected by filtration. ^{1}H NMR (400 MHz, 298 K, CD_3CN): δ 8.66 (12H, s, imine), 8.42 (12H, br, 3-pyridine), 8.36 (12H, br, 4-pyridine), 7.72 (12H, br, 5-pyridine), 7.53 (12H, br, phenyl of the triamine), 7.32 (12H, br, 6-pyridine), 6.64 (12H, br, phenyl of the triamine), 5.76 (12H, br, phenyl of the triamine), 5.25 (12H, br, phenyl of the triamine), 4.97 (4H, s, methylhydroxyl at the center of the triamine). ^{13}C NMR (125 MHz, 298 K, CD_3CN): δ 177.61, 159.64, 157.43, 151.54, 148.24, 141.31, 132.91, 131.44, 82.35. Elemental analysis of $[\mathbf{3}](PF_6)_8$ (%): Calcd for $C_{148}H_{112}F_{48}Fe_4N_{24}O_4S_8P_8\cdot 10H_2O$: C, 46.13; H, 3.45; N, 8.72. Found: C, 46.31; H, 3.24; N, 8.42.

Preparation of [Cyclohexane⊂4](NTf$_2$)$_8$. To a Teflon-capped J-Young NMR tube were added **C** (2.34 mg, 6.66 μmol, 4 equiv), 2-formylpyridine (1.90 μL, 20 μmol, 12 equiv), iron(II) triflamide dihydrate (16.5 mg, 9.99 μmol, 6 equiv), cyclohexane (10 μL, 92.5 μmol, 56.0 equiv), and deuterated acetonitrile (0.7 mL). The solution was degassed by three evacuation/nitrogen-fill cycles. The tube was kept at 50 °C overnight. ^{1}H NMR (CD_3CN): δ 10.03 (12H, s, imine), 8.90 (12H, bs, pyridine), 8.34 (12H, bs, pyridine), 8.09 (24H, bs, pyridine), 7.36 (12H, s, triamine center), 7.15 (24H, bs, triamine), 5.71 (24H, bs, triamine), −0.57 (12H, s, encapsulated cyclohexane). ^{13}C NMR (125 MHz, 298 K, CD_3CN): δ 172.54, 156.61, 156.48, 152.55, 142.59, 142.21, 140.06, 133.13, 132.78, 128.73, 127.35, 123.97, 123.31, 26.78 (free cyclohexane), 26.18 (encapsulated cyclohexane). ESI-MS: m/z 556.93 $[\mathbf{4}(NTf_2)_2(\text{cyclohexane})]^{6+}$, 724.48 $[\mathbf{4}(NTf_2)_3(\text{cyclohexane})]^{5+}$, 975.61 $[\mathbf{4}(NTf_2)_4(\text{cyclohexane})]^{4+}$, 1394.39 $[\mathbf{4}(NTf_2)_5(\text{cyclohexane})]^{3+}$.

Preparation of [5](NTf$_2$)$_8$·4C$_4$H$_8$O$_2$·0.95CH$_3$CN. To a Teflon-capped J-Young NMR tube were added **C** (5.27 mg, 0.015 mmol, 3 equiv), 2-formylpyridine (2.86 μL, 0.03 mmol, 6 equiv), iron(II) triflamide dihydrate (6.16 mg, 0.01 mmol, 2 equiv), and deuterated acetonitrile (0.5 mL). The solution was degassed by three evacuation/nitrogen-fill cycles. The tube was kept at 50 °C overnight. ^{1}H NMR (400 MHz, 323 K, CD_3CN): δ 9.40 (6H, s, imine), 8.70 (6H, d, J = 5.92 Hz, pyridine), 8.43 (6H, t, J = 7.56 Hz, pyridine), 7.96 (9H, bs, pyridine), 7.86 (6H, s, central phenyl), 7.76−7.71 (21H, m), 7.50 (6H, d, J = 8.36 Hz, triamine), 6.74 (6H, d, J = 8.16 Hz, triamine), 5.41 (24H, d, J = 7.68 Hz, triamine), 4.23 (6H, br, amine). ^{13}C NMR (125 MHz, 298 K, CD_3CN): δ 115.57, 122.48, 122.86, 122.93, 125.04, 128.92, 129.13, 129.46, 130.78, 132.07, 140.75, 141.60, 141.77, 149.46, 150.74, 156.98, 159.19, 176.09. ESI-MS: m/z 425.11 $[\mathbf{5}]^{4+}$, 660.51 $[\mathbf{5}(NTf_2)]^{3+}$, 1130.62 $[\mathbf{5}(NTf_2)_2]^{2+}$. Elemental analysis of $[\mathbf{5}](NTf_2)_8$ (%): Calcd for $C_{116}H_{81}F_{24}Fe_4N_{19}O_{16}S_8\cdot 4C_4H_8O_2\cdot 0.95CH_3CN$: C, 49.8; H, 3.31; N, 9.2. Found: C, 50.10; H 2.96; N, 8.88.

Preparation of [6](NTf$_2$)$_8$·23 H$_2$O. To a Teflon-capped J-Young NMR tube were added **D** (2.11 mg, 5.0 μmol, 4 equiv), 2-formylpyridine (1.90 μL, 20 μmol, 12 equiv), iron(II) triflamide dihydrate (2.65 mg, 7.5 μmol, 4.8 equiv), and deuterated acetonitrile (0.5 mL). The solution was degassed by three evacuation/nitrogen-fill cycles. The tube was kept at 50 °C overnight. ^{1}H NMR (400 MHz, 298 K, CD_3CN): δ 10.48 (12H, bs, imine), 9.01 (12H, d, J = 6.9 Hz, pyridine), 8.54 (12H, d, J = 6.2 Hz, pyridine), 8.32 (12H, t, J = 7.6 Hz, pyridine), 8.25 (12H, bs, pyridine), 7.67 (12H, s, triamine center), 7.43 (24H, d, J = 7.9 Hz, triamine), 5.37 (24H, d, J = 8.0 Hz, triamine). ^{13}C NMR (125 MHz, 298 K, CD_3CN): δ 174.84, 158.3, 155.91, 150.28, 143.16, 139.73, 132.48, 131.54, 131.27, 130.16, 122.17, 90.10, 89.27. ESI-MS: m/z 373.25 $[\mathbf{6}]^{8+}$, 447.90 $[\mathbf{6}(NTf_2)]^{7+}$, 547.38 $[\mathbf{6}(NTf_2)_2]^{6+}$, 686.90 $[\mathbf{6}(NTf_2)_3]^{5+}$, 895.43 $[\mathbf{6}(NTf_2)_4]^{4+}$, 1243.49 $[\mathbf{6}(NTf_2)_5]^{3+}$. Elemental analysis of $[\mathbf{6}](NTf_2)_8$ (%): Calcd for $C_{208}H_{120}F_{48}Fe_4N_{34}O_{32}S_{16}\cdot 23.1H_2O$: C, 44.05; H, 2.95; N, 8.4. Found: C, 43.86; H, 2.55; N, 7.94.

Preparation of [7](NTf$_2$)$_8$·3.3H$_2$O. To a Teflon-capped J-Young NMR tube were added **D** (2.12 mg, 5.0 μmol, 3 equiv), 2-formylpyridine (0.95 μL, 10.0 μmol, 6 equiv), iron(II) triflamide dihydrate (2.17 mg, 3.33 μmol, 2 equiv), and deuterated acetonitrile (0.5 mL). The solution was degassed by three evacuation/nitrogen-fill cycles. The tube was kept at 50 °C overnight. ^{1}H NMR (400 MHz, 298 K, CD_3CN): δ 8.92 (12H, s, imine), 8.54 (12H, d, J = 7.7 Hz, pyridine), 8.38 (12H, t, J = 8.8 Hz, pyridine), 7.78 (24H, bt, J = 7.2 Hz, pyridine), 7.64 (12H, s, triamine center), 7.47−7.40 (36H, m, pyridine and triamine), 7.27 (12H, d, J = 8.4 Hz, triamine), 6.63 (12H, d, J = 8.4 Hz, triamine), 5.33 (24H, m, triamine), 4.54 (12H, s, free NH_2). ^{13}C NMR (125 MHz, 298 K, CD_3CN): δ 176.51, 159.39, 157.54, 151.87, 150.85, 141.37, 134.79, 134.49, 134.25, 133.23, 131.80, 127.04, 125.21, 124.50, 123.39, 122.76, 115.67, 110.98, 94.11, 90.83, 90.53, 86.41. ESI-MS: m/z 479.4 $[\mathbf{7}]^{4+}$, 732.5 $[\mathbf{7}(NTf_2)]^{3+}$. Elemental analysis of $[\mathbf{7}](NTf_2)_8$ (%): Calcd for $C_{134}H_{81}F_{24}Fe_4N_{19}O_{16}S_8\cdot 3.3H_2O$: C, 51.97; H, 2.85; N, 8.59. Found: C, 51.89; H, 2.93; N, 8.69.

Crystallography. Data for **1** and **2** were collected on a Bruker-Nonius APEX2-X8-FR591 diffractometer employing confocal-mirror-monochromatized Mo Kα radiation generated from a rotating anode (0.71073 Å) with ω and ψ scans at 120(2) K.[102] Data for **3** were collected on a Nonius Kappa FR590 diffractometer employing graphite-monochromatized Mo Kα radiation generated from a sealed tube (0.71073 Å) with ω and ψ scans at 180(2) K.[102] Data integration and reduction were undertaken with S HKL Denzo and Scalepack.[102,103] Subsequent computations were carried out using the WinGX-32 graphical user interface.[104] Structures were solved by direct methods using SIR97.[105] Multiscan empirical absorption corrections were applied to the data set using SADABS[106] or SORTAV.[107] Data were refined and extended with SHELXL-97.[108] H atoms were refined using a riding model. The crystals in each case diffracted poorly and rapidly suffered solvent loss. Despite rapid handling times and a low collection temperature, the quality of the data was less than ideal (~0.84 Å resolution for **1**, ~0.95 Å for **2**, and ~1 Å for **3**). Numerous rigid-body restraints and thermal parameter constraints were required in the phenyl and pyridyl rings. Nevertheless, the quality of the data was more than sufficient to establish the connectivity of the structures. In **2**, one of the amines was disordered over two equal occupancy positions. In each structure there was a significant region of disordered anions and solvent molecules that could not be successfully modeled. In **1** and **2**, this included all of the triflate anions, while in **3**, five of the PF_6 anions could be located and were modeled. The SQUEEZE function of PLATON[109] was employed to remove the contribution of the electron density associated with these disordered anions and solvent from the model,

which resulted in far more satisfactory residuals. In each case, the electron density has been included in the reported formulas as an appropriate number of anions and solvent molecules. The crystallographic data are summarized below:

1·*8OTf*·*27MeCN*. Formula $C_{206}H_{189}F_{24}Fe_4N_{55}O_{24}S_8$, M = 4755.00; monoclinic, space group $P2_1/n$ (No. 14); a = 19.6303(12) Å, b = 32.402(2) Å, c = 30.4210(17) Å, β 95.494(2)°; V = 19 261(2) Å^3, D_{calcd} = 1.640 g cm^{-3}, Z = 4; crystal size, 0.26 mm × 0.1 mm × 0.04 mm; color, dark-red; habit, Lath; temperature = 120(2) K, λ(Mo Kα) = 0.71073 Å, μ(Mo Kα) = 0.494 mm^{-1}, T(SADABS)$_{min,max}$ = 0.786144, 1.00000, $2\theta_{max}$ = 45.00°; *hkl* ranges: −21 to 21, −34 to 34, −32 to 32; N = 104 874, N_{ind} = 24 828 (R_{merge} = 0.1399), N_{obs} = 323 [$I > 2\sigma(I)$], N_{var} = 1351; residuals: $R_1(F)$ = 0.1190, $wR_2(F^2)$ = 0.3281; GoF(all) = 0.899; $\Delta\rho_{min,max}$ = −0.509, 2.609 e Å^{-3}.

2·*4OTf*·*9MeCN*. Formula $C_{102}H_{99}F_{12}Fe_2N_{27}O_{12}S_4$, M = 2363.02; monoclinic, space group $P2_1/n$ (No. 14); a = 23.5800(10) Å, b = 18.0061(7) Å, c = 24.9071(10) Å, β 102.965(2)°; V = 10 305.6(7) Å^3, D_{calcd} = 1.523 g cm^{-3}, Z = 4; crystal size, 0.26 mm × 0.07 mm × 0.03 mm; color, dark-red; habit, blade; temperature = 120(2) K, λ(Mo Kα) = 0.71073 Å, μ(Mo Kα) = 0.461 mm^{-1}, T(SADABS)$_{min,max}$ = 0.708930, 1.00000, $2\theta_{max}$ = 50.00°; *hkl* ranges: −28 to 26, −21 to 21, −29 to 29; N = 68 799, N_{ind} = 17 936 (R_{merge} = 0.1164), N_{obs} = 6550 [$I > 2\sigma(I)$], N_{var} = 979; residuals: $R_1(F)$ = 0.1318, $wR_2(F^2)$ = 0.3715; GoF(all) = 0.939; $\Delta\rho_{min,max}$ = −0.466, 1.306 e Å^{-3}.

3·*8PF$_6$*·*5MeCN*·*5C$_4$H$_{10}$O*. Formula $C_{178}H_{177}F_{48}Fe_4N_{29}O_9P_8$, M = 4249.65; monoclinic, space group *Cc* (No. 9); a = 34.078(7) Å, b = 31.506(6) Å, c = 20.330(4) Å, β = 104.03(3)°; V = 21 176(7) Å^3, D_{calcd} = 1.333 g cm^{-3}, Z = 4; crystal size, 0.40 mm × 0.20 mm × 0.15 mm; color, purple; habit, needle; temperature = 180(2) K, λ(Mo Kα) = 0.71073 Å, μ(Mo Kα) = 0.429 mm^{-1}, T(SORTAV)$_{min,max}$ = 0.377, 0.909, $2\theta_{max}$ = 37.70°; *hkl* ranges: −30 to 30, −28 to 28, −18 to 18; N = 35 998, N_{ind} = 14 284 (R_{merge} = 0.0793), N_{obs} = 11 810 [$I > 2\sigma(I)$], N_{var} = 991; residuals: $R_1(F)$ = 0.1078, $wR_2(F^2)$ = 0.2733; GoF(all) = 1.402; $\Delta\rho_{min,max}$ = −0.700, 0.539 e Å^{-3}.

■ ASSOCIATED CONTENT

Supporting Information. Characterization of $Fe_4L_4^{8+}$ capsules and $Fe_2L_3^{4+}$ helicates (including ^{1}H NMR and ESI-MS spectra), characterization of host−guest complexes, details of the calculation of the volumes of the capsules, details of guest binding investigations, and CIFs for **1**−**3**. This material is available free of charge via the Internet at http://pubs.acs.org. The crystallographic data for **1**−**3** have also been deposited with the Cambridge Crystallographic Data Centre as entries CCDC 838411−838413.

■ AUTHOR INFORMATION

Corresponding Author

jrn34@cam.ac.uk

Present Addresses

[†]National Institute of Science Education and Research, Institute of Physics Campus, P.O. Sainik School Bhubaneswar, Orissa 751 005, India.

■ ACKNOWLEDGMENT

This work was supported by Schlumberger—Faculty for the Future Fellowship, the Marie Curie Incoming International Fellowship Scheme of the 7th EU Framework Program, and the U.K. Engineering and Physical Sciences Research Council (EPSRC). We thank the EPSRC Mass Spectrometry Service at Swansea for FT-ICR MS experiments and the National Crystallography Service at Southampton for collecting X-ray data.

■ REFERENCES

(1) Chakrabarty, R.; Mukherjee, P. S.; Stang, P. J. *Chem. Rev.* 2011, *111*, 6810.
(2) Ward, M. D. *Chem. Commun.* **2009**, 4487.
(3) Dalgarno, S. J.; Power, N. P.; Atwood, J. L. *Coord. Chem. Rev.* **2008**, *252*, 825.
(4) Fujita, M.; Tominaga, M.; Hori, A.; Therrien, B. *Acc. Chem. Res.* **2005**, *38*, 369.
(5) Tranchemontagne, D. J.; Ni, Z.; O'Keeffe, M.; Yaghi, O. M. *Angew. Chem., Int. Ed.* **2008**, *47*, 5136.
(6) Seidel, S. R.; Stang, P. J. *Acc. Chem. Res.* **2002**, *35*, 972.
(7) Ghosh, K.; Hu, J.; White, H. S.; Stang, P. J. *J. Am. Chem. Soc.* **2009**, *131*, 6695.
(8) Zheng, Y.-R.; Zhao, Z.; Kim, H.; Wang, M.; Ghosh, K.; Pollock, J. B.; Chi, K.-W.; Stang, P. J. *Inorg. Chem.* **2010**, *49*, 10238.
(9) Jin, P.; Dalgarno, S. J.; Atwood, J. L. *Coord. Chem. Rev.* **2010**, *254*, 1760.
(10) Lusby, P. J.; Müller, P.; Pike, S. J.; Slawin, A. M. Z. *J. Am. Chem. Soc.* **2009**, *131*, 16398.
(11) Riddell, I. A.; Smulders, M. M. J.; Clegg, J. K.; Nitschke, J. R. *Chem. Commun.* **2011**, *47*, 457.
(12) Custelcean, R.; Remy, P.; Bonnesen, P. V.; Jiang, D.-e.; Moyer, B. A. *Angew. Chem., Int. Ed.* **2008**, *47*, 1866.
(13) Glasson, C. R. K.; Clegg, J. K.; McMurtrie, J. C.; Meehan, G. V.; Lindoy, L. F.; Motti, C. A.; Moubaraki, B.; Murray, K. S.; Cashion, J. D. *Chem. Sci.* **2011**, *2*, 540.
(14) Huerta, E.; Metselaar, G. A.; Fragoso, A.; Santos, E.; Bo, C.; de Mendoza, J. *Angew. Chem., Int. Ed.* **2007**, *46*, 202.
(15) Kishi, N.; Li, Z.; Yoza, K.; Akita, M.; Yoshizawa, M. *J. Am. Chem. Soc.* **2011**, *133*, 11438.
(16) Meng, W.; Breiner, B.; Rissanen, K.; Thoburn, J. D.; Clegg, J. K.; Nitschke, J. R. *Angew. Chem., Int. Ed.* **2011**, *50*, 3479.
(17) Yoshizawa, M.; Klosterman, J. K.; Fujita, M. *Angew. Chem., Int. Ed.* **2009**, *48*, 3418.
(18) Furusawa, T.; Kawano, M.; Fujita, M. *Angew. Chem., Int. Ed.* **2007**, *46*, 5717.
(19) Yoshizawa, M.; Kusukawa, T.; Fujita, M.; Yamaguchi, K. *J. Am. Chem. Soc.* **2000**, *122*, 6311.
(20) Mal, P.; Breiner, B.; Rissanen, K.; Nitschke, J. R. *Science* **2009**, *324*, 1697.
(21) Leeland, J. W.; White, F. J.; Love, J. B. *J. Am. Chem. Soc.* **2011**, *133*, 7320.
(22) Cram, D. J. *Nature* **1992**, *356*, 29.
(23) Murase, T.; Horiuchi, S.; Fujita, M. *J. Am. Chem. Soc.* **2010**, *132*, 2866.
(24) Yoshizawa, M.; Tamura, M.; Fujita, M. *Science* **2006**, *312*, 251.
(25) Pluth, M. D.; Bergman, R. G.; Raymond, K. N. *Science* **2007**, *316*, 85.
(26) Fujita, M.; Oguro, D.; Miyazawa, M.; Oka, H.; Yamaguchi, K.; Ogura, K. *Nature* **1995**, *378*, 469.
(27) Caulder, D. L.; Powers, R. E.; Parac, T. N.; Raymond, K. N. *Angew. Chem., Int. Ed.* **1998**, *37*, 1840.
(28) Caulder, D. L.; Brückner, C.; Powers, R. E.; Koenig, S.; Parac, T. N.; Leary, J. A.; Raymond, K. A. *J. Am. Chem. Soc.* **2001**, *123*, 8923.
(29) Hamacek, J.; Bernardinelli, G.; Filinchuk, Y. *Eur. J. Inorg. Chem.* **2008**, 3419.
(30) Wang, J.; He, C.; Wu, P.; Wang, J.; Duan, C. *J. Am. Chem. Soc.* **2011**, *133*, 12402.
(31) Albrecht, M.; Janser, I.; Burk, S.; Weis, P. *Dalton Trans.* **2006**, 2875.
(32) Amoroso, A. J.; Jeffery, J. C.; Jones, P. L.; McCleverty, J. A.; Thornton, P.; Ward, M. D. *Angew. Chem., Int. Ed. Engl.* **1995**, *34*, 1443.
(33) Brückner, C.; Powers, R. E.; Raymond, K. N. *Angew. Chem., Int. Ed.* **1998**, *37*, 1837.

(34) Saalfrank, R. W.; Glaser, H.; Demleitner, B.; Hampel, F.; Chowdhry, M. M.; Schunemann, V.; Trautwein, A. X.; Vaughan, G. B. M.; Yeh, R.; Davis, A. V.; Raymond, K. N. *Chem.—Eur. J.* **2002**, *8*, 493.
(35) Albrecht, M.; Janser, I.; Runsink, J.; Raabe, G.; Weis, P.; Froehlich, R. *Angew. Chem., Int. Ed.* **2004**, *43*, 6662.
(36) Albrecht, M.; Ingo, J. A.; Frohlich, R. *Chem. Commun.* **2005**, 157.
(37) Granzhan, A.; Riis-Johannessen, T.; Scopelliti, R.; Severin, K. *Angew. Chem., Int. Ed.* **2010**, *49*, 5515.
(38) Granzhan, A.; Schouwey, C.; Riis-Johannessen, T.; Scopelliti, R.; Severin, K. *J. Am. Chem. Soc.* **2011**, *133*, 7106.
(39) Liu, Y.; Lin, Z.; He, C.; Zhao, L.; Duan, C. *Dalton Trans.* **2010**, *39*, 11122.
(40) Campbell, V. E.; Nitschke, J. R. *Synlett* **2008**, 2077.
(41) Rowan, S. J.; Cantrill, S. J.; Cousins, G. R. L.; Sanders, J. K. M.; Stoddart, J. F. *Angew. Chem., Int. Ed.* **2002**, *41*, 898.
(42) Saalfrank, R. W.; Demleitner, B.; Glaser, H.; Maid, H.; Bathelt, D.; Hampel, F.; Bauer, W.; Teichert, M. *Chem.—Eur. J.* **2002**, *8*, 2679.
(43) Paul, R. L.; Argent, S. P.; Jeffery, J. C.; Harding, L. P.; Lynam, J. M.; Ward, M. D. *Dalton Trans.* **2004**, 3453.
(44) Argent, S. P.; Riis-Johannessen, T.; Jeffery, J. C.; Harding, L. P.; Ward, M. D. *Chem. Commun.* **2005**, 4647.
(45) Glasson, C. R. K.; Meehan, G. V.; Clegg, J. K.; Lindoy, L. F.; Turner, P.; Duriska, M. B.; Willis, R. *Chem. Commun.* **2008**, 1190.
(46) Tidmarsh, I. S.; Taylor, B. F.; Hardie, M. J.; Russo, L.; Clegg, W.; Ward, M. D. *New J. Chem.* **2009**, *33*, 366.
(47) Ward, M. D. *Chem. Commun.* **2009**, 4487.
(48) Houk, K. N.; Leach, A. G.; Kim, S. P.; Zhang, X.-Y. *Angew. Chem., Int. Ed.* **2003**, *42*, 4872.
(49) Yeh, R. M.; Xu, J.; Seeber, G.; Raymond, K. N. *Inorg. Chem.* **2005**, *44*, 6228.
(50) El Aroussi, B.; Guenee, L.; Pal, P.; Hamacek, J. *Inorg. Chem.* **2011**, *50*, 8588.
(51) Albrecht, M.; Janser, I.; Meyer, S.; Weis, P.; Froehlich, R. *Chem. Commun.* **2003**, 2854.
(52) Saalfrank, R. W.; Maid, H.; Scheurer, A.; Heinemann, F. W.; Puchta, R.; Bauer, W.; Stern, D.; Stalke, D. *Angew. Chem., Int. Ed.* **2008**, *47*, 8941.
(53) Li, F.; Clegg, J. K.; Lindoy, L. F.; MacQuart, R. B.; Meehan, G. V. *Nat. Commun.* **2011**, *2*, 205.
(54) Albrecht, M.; Schneider, M.; Rottele, H. *Chem. Ber. Recl.* **1997**, *130*, 615.
(55) Glasson, C. R. K.; Meehan, G. V.; Clegg, J. K.; Lindoy, L. F.; Smith, J. A.; Keene, F. R.; Motti, C. *Chem.—Eur. J.* **2008**, *14*, 10535.
(56) Kleywegt, G. J.; Jones, T. A. *Acta Crystallogr.* **1994**, *D50*, 178.
(57) Saalfrank, R. W.; Maid, H.; Scheurer, A.; Puchta, R.; Bauer, W. *Eur. J. Inorg. Chem.* **2010**, 2903.
(58) *CAChe WorkSystem Pro*; Fujitsu Limited: Beaverton, Oregon, 2000−2006.
(59) Wu, A. X.; Isaacs, L. *J. Am. Chem. Soc.* **2003**, *125*, 4831.
(60) Caulder, D. L.; Raymond, K. N. *Angew. Chem., Int. Ed. Engl.* **1997**, *36*, 1440.
(61) Hwang, I.-W.; Kamada, T.; Ahn, T. K.; Ko, D. M.; Nakamura, T.; Tsuda, A.; Osuka, A.; Kim, D. *J. Am. Chem. Soc.* **2004**, *126*, 16187.
(62) Jiang, W.; Winkler, H. D. F.; Schalley, C. A. *J. Am. Chem. Soc.* **2008**, *130*, 13852.
(63) Rang, A.; Nieger, M.; Engeser, M.; Lutzen, A.; Schalley, C. A. *Chem. Commun.* **2008**, 4789.
(64) Zheng, Y. R.; Yang, H. B.; Northrop, B. H.; Ghosh, K.; Stang, P. J. *Inorg. Chem.* **2008**, *47*, 4706.
(65) Rekharsky, M. V.; Yamamura, H.; Ko, Y. H.; Selvapalam, N.; Kim, K.; Inoue, Y. *Chem. Commun.* **2008**, 2236.
(66) Jolliffe, K. A.; Timmerman, P.; Reinhoudt, D. N. *Angew. Chem., Int. Ed.* **1999**, *38*, 933.
(67) Deeming, A. J.; Hogarth, G.; Lee, M.-y.; Saha, M.; Redmond, S. P.; Phetmung, H.; Orpen, A. G. *Inorg. Chim. Acta* **2000**, *309*, 109.
(68) Conerney, B.; Jensen, P.; Kruger, P. E.; MacGloinn, C. *Chem. Commun.* **2003**, 1274.
(69) Hansch, C.; Leo, A.; Taft, R. W. *Chem. Rev.* **1991**, *91*, 165.
(70) Hristova, Y. R.; Smulders, M. M. J.; Clegg, J. K.; Breiner, B.; Nitschke, J. R. *Chem. Sci.* **2011**, *2*, 638.
(71) Schultz, D.; Nitschke, J. R. *J. Am. Chem. Soc.* **2006**, *128*, 9887.
(72) Clegg, J. K.; Li, F.; Jolliffe, K. A.; Meehan, G. V.; Lindoy, L. F. *Chem. Commun.* **2011**, *47*, 6042.
(73) Glasson, C. R. K.; Meehan, G. V.; Motti, C. A.; Clegg, J. K.; Turner, P.; Jensen, P.; Lindoy, L. F. *Dalton Trans.* **2011**, *40*, 10481.
(74) Meng, W.; Clegg, J. K.; Thoburn, J. D.; Nitschke, J. R. *J. Am. Chem. Soc.* **2011**, *133*, 13652.
(75) Caulder, D. L.; Raymond, K. N. *Dalton Trans.* **1999**, 1185.
(76) Albrecht, M. *Chem.—Eur. J.* **2000**, *6*, 3485.
(77) Albrecht, M.; Schneider, M. *Chem. Commun.* **1998**, 137.
(78) Hennrich, G.; Anslyn, E. V. *Chem.—Eur. J.* **2002**, *8*, 2219.
(79) Iwamura, H.; Mislow, K. *Acc. Chem. Res.* **1988**, *21*, 175.
(80) Lindquist, N. R.; Carter, T. G.; Cangelosi, V. M.; Zakharov, L. N.; Johnson, D. W. *Chem. Commun.* **2010**, *46*, 3505.
(81) Ajami, D.; Rebek, J., Jr. *Angew. Chem., Int. Ed.* **2008**, *47*, 6059.
(82) Tang, K. T.; Toennies, J. P. *J. Chem. Phys.* **1978**, *68*, 5501.
(83) Hua, Y. R.; Flood, A. H. *Chem. Soc. Rev.* **2010**, *39*, 1262.
(84) Sessler, J. L.; Camiolo, S.; Gale, P. A. *Coord. Chem. Rev.* **2003**, *240*, 17.
(85) Sambrook, M. R.; Beer, P. D.; Wisner, J. A.; Paul, R. L.; Cowley, A. R. *J. Am. Chem. Soc.* **2004**, *126*, 15364.
(86) *SPARTAN'10 for Windows*; Wavefunction, Inc: Irvine, CA, 2010.
(87) Mecozzi, S.; Rebek, J., Jr. *Chem.—Eur. J.* **1998**, *4*, 1016.
(88) Mal, P.; Schultz, D.; Beyeh, K.; Rissanen, K.; Nitschke, J. R. *Angew. Chem., Int. Ed.* **2008**, *47*, 8297.
(89) Asadi, A.; Ajami, D.; Rebek, J., Jr. *J. Am. Chem. Soc.* **2011**, *133*, 10682.
(90) Trembleau, L.; Rebek, J., Jr. *Science* **2003**, *301*, 1219.
(91) Beissel, T.; Powers, R. E.; Parac, T. N.; Raymond, K. N. *J. Am. Chem. Soc.* **1999**, *121*, 4200.
(92) Clegg, J. K.; Lindoy, L. F.; Moubaraki, B.; Murray, K. S.; McMurtrie, J. C. *Dalton Trans.* **2004**, 2417.
(93) Liao, P. H.; Langloss, B. W.; Johnson, A. M.; Knudsen, E. R.; Tham, F. S.; Julian, R. R.; Hooley, R. J. *Chem. Commun.* **2010**, *46*, 4932.
(94) Laughrey, Z.; Gibb, B. C. *Chem. Soc. Rev.* **2011**, *40*, 363.
(95) Breiner, B.; Clegg, J. K.; Nitschke, J. R. *Chem. Sci.* **2011**, *2*, 51.
(96) Frischmann, P. D.; Facey, G. A.; Ghi, P. Y.; Gallant, A. J.; Bryce, D. L.; Lelj, F.; MacLachlan, M. J. *J. Am. Chem. Soc.* **2010**, *132*, 3893.
(97) Gianneschi, N. C.; Masar, M. S.; Mirkin, C. A. *Acc. Chem. Res.* **2005**, *38*, 825.
(98) Schalley, C. A.; Lutzen, A.; Albrecht, M. *Chem.—Eur. J.* **2004**, *10*, 1072.
(99) Corbett, P. T.; Leclaire, J.; Vial, L.; West, K. R.; Wietor, J. L.; Sanders, J. K. M.; Otto, S. *Chem. Rev.* **2006**, *106*, 3652.
(100) Saur, I.; Scopelliti, R.; Severin, K. *Chem.—Eur. J.* **2006**, *12*, 1058.
(101) Chung, M.-K.; Severin, K.; Lee, S. J.; Waters, M. L.; Gagne, M. R. *Chem. Sci.* **2011**, *2*, 744.
(102) Hooft, R. W. W. *COLLECT*; Nonius BV: Delft, The Netherlands, 1998.
(103) Otwinowski, Z.; Minor, W. *Methods Enzymol.* **1997**, *276*, 307.
(104) Farrugia, L. *J. Appl. Crystallogr.* **1999**, *32*, 837.
(105) Altomare, A.; Burla, M. C.; Camalli, M.; Cascarano, G. L.; Giocavazzo, C.; Gaugliardi, A.; Moliterni, G. C.; Polidori, G.; Spagna, S. *J. Appl. Crystallogr.* **1999**, *32*, 115.
(106) Sheldrick, G. M. *SADABS: Empirical Absorption and Correction Software*; University of Göttingen: Göttingen, Germany, 1996−2008.
(107) Blessing, R. H. *Acta Crystallogr.* **1995**, *A51*, 33.
(108) Sheldrick, G. M. *SHELX-97: Programs for Crystal Structure Analysis*; University of Göttingen: Göttingen, Germany, 1997.
(109) Spek, A. L. *PLATON: A Multipurpose Crystallographic Tool*; Utrecht University: Utrecht, The Netherlands, 2008.